Alteration of performance in a mouse model of Emery-Dreifuss muscular dystrophy caused by A-type lamins gene mutation

Rémi Thomasson[1], Nicolas Vignier[2], Cecile Peccate[2], Nathalie Mougenot[3], Philippe Noirez[1,4], Antoine Muchir[2*]

[1]Université Sorbonne Paris Cité, EA7329, Université Paris Descartes, Paris, France.

[2]Sorbonne Université, INSERM UMRS974, Center of Research in Myology, Institut de Myologie, Paris, France

[3]Sorbonne Université, INSERM, UMS28 Phénotypage du petit animal, Paris F-75013, France

[4]Institute for Research in Medicine and Epidemiology of Sport, National Institute of Sport, Expertise and Performance, Paris, France.

[*]Correspondence:
Antoine Muchir, PhD
e-mail: a.muchir@institut-myologie.org

ABSTRACT

Autosomal Emery-Dreifuss muscular dystrophy is caused by mutations in the lamin A/C gene (*LMNA*) encoding A-type nuclear lamins, intermediate filament proteins of the nuclear envelope. Classically, the disease manifests as scapulo-humero-peroneal muscle wasting and weakness, early joint contractures and dilated cardiomyopathy with conduction blocks; however, variable skeletal muscle involvement can be present. Previously, we and other demonstrated altered activity of signaling pathways in hearts and striated muscles of $Lmna^{H222P/H222P}$ mice, a model of autosomal Emery-Dreifuss muscular dystrophy. We showed that blocking their activation improved cardiac function. However, the evaluation of the benefit of these treatments on the whole organism is suffering from a better knowledge of the performance in mouse models. We show in the present study that $Lmna^{H222P/H222P}$ mice display a significant loss of lean mass, consistent with the dystrophic process. This is associated with altered VO_2 peak and respiratory exchange ratio (RER). These results showed for the first time that $Lmna^{H222P/H222P}$ mice have decreased performance and provided a new useful means for future therapeutic interventions on this model of Emery-Dreifuss muscular dystrophy.

Keywords: Emery-Dreifuss muscular dystrophy, lamin, nuclear envelope, *LMNA*, performance

INTRODUCTION

LMNA mutations cause an autosomal dominant inherited form of Emery-Dreifuss muscular dystrophy (EDMD) (1). EDMD is characterized by the clinical triad of joint contractures that begin in early childhood, slowly progressive muscle weakness and wasting initially in a humero-peroneal distribution that later extends to the scapular and pelvic girdle muscles, and cardiac involvement that manifests as poor exercise tolerance, and congestive heart failure (2,3). Clinical variability ranges from early onset with severe presentation in childhood to late onset with slow progression in adulthood. Cardiac involvement usually occurs after the second decade (4). *LMNA* encodes the A-type nuclear lamins (5), which arise from alternative RNA splicing and are the constituents of nuclear lamina. Given the ability of mouse models to phenocopy various aspects of cardiovascular diseases, the use of mouse models has become critical to the study of cardiac biology, physiology, and novel therapeutics prior to translating findings to human. We largely contributed in understanding the metabolic and physiological mechanisms regulating cardiac function and energy balance in EDMD, both in animal models and in patient's tissues. These include abnormal regulation of the mitogen-activated protein kinase (MAPK) signaling cascade (6,7), altered actin dynamics (8), altered Wnt/β-catenin signaling (9), fibrosis (10), NAD signaling (11) and AKT/mTOR signaling (12). Despite the growing understanding of the pathogenesis of EDMD as well as the discovery of novel therapeutic for the disease (7,9-13), little is known on the overall benefit of these treatments on the performance of the animals. There is a need for more comprehensive ways of assessing disease progression and treatment efficacy. Traditional approaches to monitoring disease progression in preclinical models of muscular dystrophies are limited mostly to histological analyses and functional measurements of single fibers or muscle groups. However, none of these tests can assess systemic muscle function in a non-invasive approach consistent with clinical assessment in EDMD patients.

Respiration is a product of systemic skeletal and cardiac muscle function (14). We here hypothesized that quantifying respiration during exercise would be a mean to studying systemic muscle function in a mouse model of EDMD, as it is commonly used to assess performance in humans (15). During testing, cardiac output primarily drives the associated increase in oxygen consumption (VO_2) until peak oxygen consumption (VO_2 peak) and exhaustion is achieved. Combined

measurements of exercise, respiratory performance and histological marker expression therefore provide a comprehensive, reliable, and powerful mean for assessing drug efficacy in a mouse model for EDMD, which in turn could help advance drug discovery.

RESULTS

Depressed left ventricular function in *Lmna*$^{H222P/H222P}$ mouse model

To explore the role of A-type lamins in the development of EDMD, we studied a mouse model that display a *Lmna* mutation changing the histidine in position 222 into a proline (15). We used transthoracic echocardiography to determine the cardiac function of *Lmna*$^{H222P/H222P}$ male mice. While the cardiac structure and function were not statistically different at 3 months of age, at 6 months of age, *Lmna*$^{H222P/H222P}$ male mice have increased left ventricular diameters, and decreased fractional shortening (FS) compared with wild type animals (Figure 1A) (8,9,16). Left ventricular dilatation in *Lmna*$^{H222P/H222P}$ male mice at 6 months of age was demonstrated by histopathological analysis (Figure 1B). M-mode transthoracic echocardiography showed increased left ventricular end-systolic and end-diastolic diameters in *Lmna*$^{H222P/H222P}$ mice compared with wild type mice (Figure 1B). We showed a marked increased of myocardial fibrosis in heart from *Lmna*$^{H222P/H222P}$ male mice at 6 months of age, as observed by Sirius Red staining (Figure 1C).

Alteration of body composition in *Lmna*$^{H222P/H222P}$ mouse model

As the EDMD progresses further, skeletal muscle continues to be lost, which can result in weight loss. We assessed the body composition using DEXA lean/fat in *Lmna*$^{H222P/H222P}$ mice. We observed that *Lmna*$^{H222P/H222P}$ mice have a significant difference in body weight compared with wild type mice (Figure 2A). In 3-month-old *Lmna*$^{H222P/H222P}$ mice, the mean of body weight was 24.12g, while from wild type mice it was 26.66g. At 6 months of age, the mean of body weight was 24.94g for *Lmna*$^{H222P/H222P}$ mice, while it was 28.14g for wild type mice. Further complicating these issues are the changes in body composition that are linked to EDMD. We observed that *Lmna*$^{H222P/H222P}$ mice have markedly increased body fat mass and relative body fat mass (Figure 2B, 2C) and reduced body lean mass and relative body lean mass (Figure 2B, 2C) compared with wild type mice. The

loss of lean mass was consistent with the dystrophic process (Figure 3A, 3B) and the increase in adiposity could result from the decreased activity associated with the loss of activity.

Alteration of physical performance in *Lmna*$^{H222P/H222P}$ mouse model

We therefore asked whether we could assess the activity of *Lmna*$^{H222P/H222P}$ mice. Forced exercise on a treadmill was used to measure VO_2 peak. The VO_2 peak corresponds to both the cardiovascular system's functional limitation and the organism's aerobic capacity. Peak oxygen consumption has been previously validated to assess prognosis in patients with heart failure (17). We showed that *Lmna*$^{H222P/H222P}$ mice have a significant reduction in VO_2 peak, as well as relative VO_2 peak, compared with wild type mice at 3 and 6 months of age (Figure 4A). The ratio VCO_2/VO_2 is the respiratory exchange ratio (RER), which can be used to determine the proportion of carbohydrates and fatty acid utilized during an activity. Peak RER has been used as an objective parameter of effort (18). The *Lmna*$^{H222P/H222P}$ mice have a significant decreased RER at VO_2 peak (Figure 4B). The lower RER at VO_2 peak observed in *Lmna*$^{H222P/H222P}$ male mice indicates a higher level of lipid metabolism when compared with wild type mice. Importantly, there was a significant difference in the maximal speed and the running distance between the two genotypes (Figure 5); thus, the decreased metabolic performance of *Lmna*$^{H222P/H222P}$ mice resulted to a change in physical activity.

We next tested whether interventions on mice could alter these parameters of effort. Given that the NAD^+ precursor - nicotinamide riboside (NR) supplemented diet was recently shown to have benefit on cardiac contractility in *Lmna*$^{H222P/H222P}$ mice (11), we next assessed in a pilot study the NR effect on physical and metabolic performances in *Lmna*$^{H222P/H222P}$ male mice. Since we recently reported an aberrant cardiac NAD^+ content, we first assessed the steady-state skeletal muscle (soleus) NAD^+ level in both male wild type and *Lmna*$^{H222P/H222P}$ mice. We showed that the NAD^+ content was significantly lowered in hearts from *Lmna*$^{H222P/H222P}$ mice at 6 months of age compared with wild type mice, when the structure of soleus was altered (symptomatic) (Figure 6A). We next assessed the expression level of enzymes from the salvage pathway of NAD^+ biosynthesis by real-time PCR using RNA extracted from *Lmna*$^{H222P/H222P}$ mouse soleus at 6 months of age. There was a significant

increased *Nmrk2* mRNA expression in the soleus of *Lmna*$^{H222P/H222P}$ mice compared with wild type mice (Figure 6B). We showed that feeding *Lmna*$^{H222P/H222P}$ mice with NR, the substrate for Nmrk2, for 2 months improved significantly RER at VO_2 peak compared with chow diet-fed mice (Figure 6C). We also reported a significant difference in the maximal speed and the distance between the NR-fed and the chow diet-fed groups (Figure 6D). Taken together these results showed, that RER at VO_2 peak as well as physical performance are reflecting a partially restoration of the striated muscle structure and function and could therefore be used to assess future benefit of treatment in mouse model of EDMD.

DISCUSSION

There is an important need for a more comprehensive approach to evaluate the efficacy of therapeutics for neuromuscular diseases. Although traditional measures of disease pathology are useful, they have a limited functionality given that they do not assess the whole body. Muscle disease is usually assessed by histological analysis and circulating markers of myofiber injury or functional assessments of isolated muscles. Our findings strongly suggest that non-invasive protocols for assessing exercise performance in *Lmna*$^{H222P/H222P}$ mice quantifying several parameters of respiration and exercise are useful to assess the dystrophic pattern in EDMD. Exercise performance (e.g. 6 minutes walk-test) was recently used as the primary endpoint to assess the benefit of p38 inhibitor ARRY-797 (7) in patients with cardiomyopathy caused by *LMNA* mutation (ClinicalTrials.gov Identifier: NCT02057341). This clinical trial showed that patients receiving ARRY-797 performed better, with a mean change from baseline, of 69 meters.

Measures of respiratory performance during exercise have been established for other animal model of muscular dystrophy (19), but are lacking for mouse models of EDMD mice. We showed that respiratory performance was impaired in *Lmna*$^{H222P/H222P}$ mice. Our findings illustrate the usefulness of respiratory performance in quantifying the dystrophic phenotype in EDMD, as differences in several exercise parameters (e.g., VO_2 peak, RER) were detected even before detection of dystrophic pattern by histological analysis. Thus, quantifying respiratory performance during exercise is in some ways a

more sensitive means for assessing muscular dystrophy in a mouse model for EDMD. The unique patterns of VO_2 peak and RER in exercising *Lmna*$^{H222P/H222P}$ mice identified novel and very useful markers for assessing exercise performance. Our findings would benefit the investigational drugs that could correct loss of skeletal muscle and could ameliorate performance in EDMD. Along these lines, we showed that interventional treatment using nicotinamide riboside (NR) significantly improved RER at VO_2 peak in *Lmna*$^{H222P/H222P}$ mice.

The RER is defined as the CO_2 produced/O_2 consumed. This ratio increases with the exercise intensity and is commonly used to indirectly determine the relative contribution of carbohydrate and lipids to overall energy expenditure. In *Lmna*$^{H222P/H222P}$ mice, we showed a decreased RER compared with wild type mice, indicating greater reliance on fatty acid oxidation. It has long been recognized that substrate metabolism is altered in the heart that undergoes pathological conditions (20). We recently reported a marked decrease of pyruvate to lactate exchange kinetics in the heart muscle from *Lmna*$^{H222P/H222P}$ mice (21). Moreover, we recently reported a cardiac muscle nicotinamide adenine dinucleotide (NAD^+) depletion in *Lmna*$^{H222P/H222P}$ mice (9), suggesting a decreased activity of the pyruvate dehydrogenase complex and a reduced production of acetyl coenzyme A from carbohydrates. It would be interesting to extensively perform metabolomics studies in these mice to address the primary metabolic defect, which lead to decline in the function.

Assessing respiration (VO_2 and VCO_2) during exercise greatly increases the overall understanding of disease pathology, as it examines the combination of cardiac and skeletal muscle functions. Taken together, our study suggests that the use of respiratory performance during exercise to quantify changes in the dystrophic phenotype is a good complement to histological markers. Indeed, it can provide non-invasive markers for assessing EDMD disease progression, which is not always reflected histologically. The phenotypic changes observed in *Lmna*$^{H222P/H222P}$ mice can now be used to guide future interventional therapies to assess their beneficial effect.

ACKNOWLEDGEMENTS

This study was supported by funds from the Association Française contre les Myopathies, from the Institut National de la Santé et de la Recherche Médicale, Sorbonne Université and Agence Nationale de la Recherche (ANR-17-CE17-0015-03). The authors gratefully acknowledge ChromaDex for providing NR. P.M. was supported by Région Ile de France and by labex GR-Ex. The labex GR-Ex, reference ANR-11-LABX-0051 is funded by the program "Investissements d'avenir" of the French National Research Agency, (ANR-11-IDEX-0005-02).

COMPETING INTERESTS

All other authors have declared no conflicts of interest.

MATERIAL AND METHODS

Mice

Lmna$^{H222P/H222P}$ mice (16) were fed chow and housed in a disease-free barrier facility at 12h/12h light/dark cycles. All animal experiments were approved by the French Ministry of Health at the Center for Research in Myology for the Care and Use of Experimental Animals. The animal experiments were performed according to the guidelines from Directive 2010/63/EU of the European Parliament on the protection of animals used for scientific purposes. Chow supplemented with 0.25% NR (400 mg/kg) (Chromadex), as previously reported (11) was formulated by Safe (Scientific Animal Food and Engineering).

Echocardiography

Mice were anesthetized with 0.75% isoflurane in O_2 and placed in a heating pad. Transthoracic echocardiography was performed using an ACUSON 128XP/10 ultrasound with an 11 MHz transducer applied to the chest wall. All parameters were measured by a "blinded echocardiographer" unaware of the genotype or treatment of the mice, performed in 2D mode and M-mode in triplicate.

Histology

Frozen pieces of soleus and diaphragm were mounted in Tissue-Tek (Fisher Scientific) and 10 µm sections cut on a cryostat. Sections were stained with hematoxylin and eosin for histological analysis. Representa-tive sections were photographed using a Microphot SA (Nikon) light microscope attached to a Spot RT Slide camera (Diagnostic Instruments). Images were processed using Adobe Photoshop CS (Adobe Systems).

qPCR analysis

Total RNA was extracted using the RNeasy Mini kit (Qiagen). cDNA was synthesized using the SuperScript III synthesis system according to the manufacturer's instructions (Invitrogen). Real-time qPCR reactions were performed with SYBR Green I Master mix (Roche) using with the LightCycler

480 (Roche). Relative levels of mRNA expression calculated using the $\Delta\Delta C_T$ method were normalized by comparison to housekeeping mRNA.

NAD^+ concentration quantification

Fresh mouse tissues were homogenized and processed according to previous report (11). The concentration of soleus NAD^+ was determined using a spectrophotometric assay as described previously (11). Absorption measurements were carried out in 96-well plates by spectrophotometry (Tecan).

Weight and body composition

The weight of the mice and their body composition (lean mass and fat mass) were measured throughout the protocol period. For body composition we used a nuclear magnetic resonance system (LF90II, Bruker, Germany).

Evaluation of the physical performance

Each mouse was evaluated on a one-way treadmill equipped with an indirect calorimetry system (Phenomaster, TSE, Germany). The performance evaluation protocol consisted of increasing the speed by 0.01 $m.s^{-1}$ every 15 seconds. Oxygen consumption (VO_2), carbon dioxide production (VCO_2) and respiratory exchange ratio (RER = VCO_2/VO_2) were recorded every second. Oxygen consumption peak ($VO_{2\ peak}$ in $ml.h^{-1}$) was set as the highest VO_2 value achieved during the test. We developed an algorithm based on the Savitzky-Golay principle (22) to automate the analysis of calorimetric data by smoothing the noisy data. The maximum speed reached by each mouse was recorded. The maximum speed corresponds to the speed at which the mouse can no longer run on the treadmill. All protocols were conducted for each mouse until exhaustion. Exhaustion was defined as the time when the animal "preferred" to receive electric stimulation through the grid installed at the beginning of the treadmill rather than continue the race. The intensity of the electric stimulation was 1.2 mA during 1s, with 1s latency. Before each protocol, there was a 3-minute acclimatization on the treadmill at low speeds

from 0.01 to 0.05 $m.s^{-1}$. All these performance measurements were realized in the "Performance & Metabolism in Mice" facility (PMM, EA7329, Paris Descartes University, Paris, France).

Statistics

Statistical analyses were performed using GraphPad Prism software. Statistical significance between groups of mice was analyzed with a corrected parametric test (Welch's *t* test), with a value of $P<0.05$ being considered significant. To validate results, we performed a non-parametric test (Wilcoxon-Mann-Whitney test). Values are represented as means ± standard errors of mean (SEM).

REFERENCES

1. Bonne, G., Di Barletta, M. R., Varnous, S., Becane, H., Hammouda, E. H., Merlini, L., et al. (1999). Mutations in the gene encoding lamin A/C cause autosomal dominant Emery-Dreifuss muscular dystrophy. *Nature Genet.* **21**, 285-288.

2. Emery, A. E. H., and Dreifuss, F. E. (1966). Unusual type of benign X- linked muscular dystrophy. *J. Neurol. Neurosurg. Psychiat.* **29**, 338-342.

3. Sanna, T., Dello Russo, A., Toniolo, D., Vytopil, M., Pelargonio, G., De Martino, G., et al. (2003). Cardiac features of Emery-Dreifuss muscular dystrophy caused by lamin A/C gene mutations. *Eur. Heart J.* **24**, 2227-2236.

4. Captur, G., Arbustini, E., Bonne, G., Syrris, P., Mills, K., Wahbi, K., Mohiddin, S.A., McKenna, W.J., Pettit, S., Ho, C.Y., Muchir, A., Gissen, P., Elliott, P.M., Moon, J.C. (2018) Lamin and the heart. *Heart* **104**, 468-479.

5. Lin, F., and Worman, H. J. (1993). Structural organization of the human gene encoding nuclear lamin A and nuclear lamin C. *J. Biol. Chem.* **268**, 16321-16326.

6. Muchir, A., Pavlidis, P., Decostre, V., Herron, A. J., Arimura, T., Bonne, G., et al. (2007). Activation of MAPK pathways links LMNA mutations to cardiomyopathy in Emery-Dreifuss muscular dystrophy. *J. Clin. Invest.* **117**, 1282-1293.

7. Muchir, A., Wu, W., Choi, J. C., Iwata, S., Morrow, J., Homma, S., et al. (2012). Abnormal p38alpha mitogen-activated protein kinase signaling in dilated cardiomyopathy caused by lamin A/C gene mutation. *Hum. Mol. Genet.* **21**, 4325-4333.

8. Chatzifrangkeskou, M., Yadin, D., Marais, T., Chardonnet, S., Cohen-Tannoudji, M., Mougenot, N., et al. (2018). Cofilin-1 phosphorylation catalyzed by ERK1/2 alters cardiac actin dynamics in dilated cardiomyopathy caused by lamin A/C gene mutation. *Hum. Mol. Genet.* **27**, 3060-3078.

9. Le Dour, C., Macquart, C., Sera, F., Homma, S., Bonne, G., Morrow, J.P, et al. (2017) Decreased Wnt/b-catenin signaling contributes to the pathogenesis of dilated cardiomyopathy caused by mutations in the lamin A/C gene. *Hum. Mol. Genet.* **26**, 333-343.

10. Chatzifrangkeskou, M., Le Dour, C., Wu, W., Morrow, J.P., Joseph, L.C., Beuvin, M., et al. (2016) ERK1/2 directly acts on CTGF/CCN2 expresssion to mediate fibrosis in cardiomyopathy caused by mutations in the lamin A/C gene. *Hum. Mol. Genet.* **25**, 2220-2233.

11. Vignier, N., Chatzifrangkeskou, M., Rodriguez, B. M., Mericskay, M., Mougenot, N., Bonne, G., et al. (2018). Rescue of biosynthesis of nicotinamide adenine dinucleotide (NAD+) protects the heart in cardiomyopathy caused by lamin A/C gene mutation. *Hum. Mol. Genet*. **27**, 3870-3880.

12. Choi, J.C., Muchir, A., Wu, W., Iwata, S., Homma, S., Morrow, J.P. and Worman, H.J. (2012) Temsirolimus activates autophagy and ameliorates cardiomyopathy caused by lamin A/C gene mutation. *Sci. Transl. Med.*, **4**, 144ra102.

13. Wu, W., Muchir, A., Shan, J., Bonne, G., and Worman, H.J. (2011) Mitogen-activated protein kinase inhibitors improve heart function and prevent fibrosis in cardiomyopathy caused by mutation in lamin A/C gene. *Circulation* **123**, 53-61.

14. Bassett, D.R. Jr, Howley, E.T. Limiting factors for maximum oxygen uptake and determinants of endurance performance. (2000) *Med. Sci. Sports Exerc.* **32**, 70-84.

15. Hoydal, M.A., Wisloff, U., Kemi, O.J., Ellingsen, O. (2007) Running speed and maximal oxygen uptake in rats and mice: practical implications for exercise training. *Eur. J. Cardiovasc. Prev.* **14**, 753-760.

16. Arimura, T., Helbling-Leclerc, A., Massart, C., Varnous, S., Niel, F., Lacène, E., Fromes, Y., Toussaint, M., Mura, A.-M., Keller, D.I. *et al.* (2005) Mouse model carrying H222P-Lmna mutation develops muscular dystrophy and dilated cardiomyopathy similar to human striated muscle laminopathies. *Hum. Mol. Genet.*, **14**, 155–169.

17. Chase, P.J., Kenjale, A., Cahalin, L.P., Arena, R., Davis, P.G., Myers, J., Guazzi, M., Forman, D.E., Ashley, E., Peberdy, M.A., West, E., Kelly, C.T. and Bensimhon, D.R. (2013) Effects of respiratory exchange ratio on the prognostic value of peak oxygen consumption and ventilator efficiency in patients with systolic heart failure. *JACC Heart Fail*. **1**, 427-432.

18. Mezzani, A., Corrà, U., Bosimini, E., Giordano, A. and Giannuzzi, P. (2003) Contribution of peak respiratory exchange ratio to peak VO2 prognostic reliability in patients with chronic heart failure and severely rduced exercise capacity. *Am. Heart J.* **145**, 1102-1107.

19. Rocco, A.B., Levalley, J.C., Eldridge, J.A., Marsh, S.A. and Rodgers, B.D. (2014) A novel protocol for assessing exercise performance and dystropathophysiology in the mdx mouse. *Muscle & Nerve* **50**, 541-548.

20. Ritterhoff, J. and Tian, R. (2017) Metabolism in cardiomyopathy: every substrate matters. *Cardiovasc. Res.* **113**, 411–421.

21. Cavallari, E., Carrera, C., Sorge, M., Bonne, G., Muchir, A., Aime, S. and Reineri, F. (2018) The ^{13}C hyperpolarized pyruvate generated by ParaHydrogen detects the response of the heart to altered metabolism in real time. *Sci. Rep.* **8**, 8366.

22. Savitzky, A. and Golay, M.J.E. (1964) Smoothing and Differentiation of Data by Simplified Least Squares Procedures. *Anal. Chem.* **36**, 1627–1639.

FIGURES

Six Figures

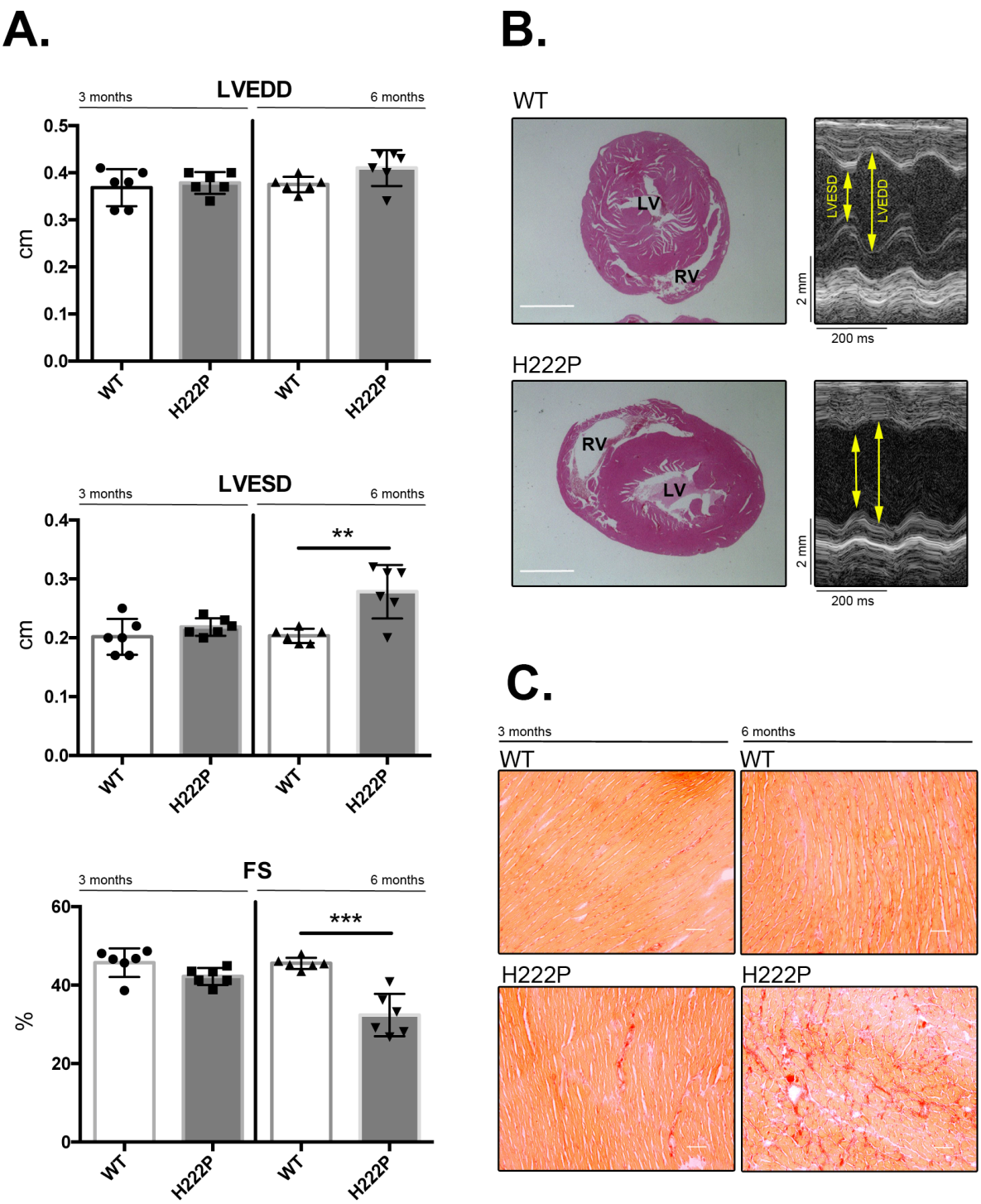

Figure 1. Alteration of left ventricular function in *Lmna*$^{H222P/H222P}$ mice

(A) Graphs showing mean left ventricular end diastolic diameter (LVEDD), mean left ventricular end systolic diameter (LVESD) and fractional shortening (FS) in 3-month-old and 6-month-old male *Lmna*$^{H222P/H222P}$ (H222P) and wild type (WT) mice (n=6). Values for each individual mouse as well SEMs of means (bars) are shown. $^{**}P<0.005$, $^{***}P<0.0005$. **(B)** Histological analysis of heart sections stained with hematoxylin and eosin from *Lmna*$^{H222P/H222P}$ (H222P) and wild type (WT) mice. Scale bar: 1mm. Transthoracic M-mode echocardiographic tracings in *Lmna*$^{H222P/H222P}$ (H222P) and wild type (WT) mice.

LV end-systolic diameter (LVESD) and LV end-diastolic diameter (LVEDD) are indicated. **(C)** Sirius Red staining of cross sections of heart from 3-month-old and 6-month-old male *Lmna*$^{H222P/H222P}$ (H222P) and wild type (WT) mice. Scale bar: 25μm.

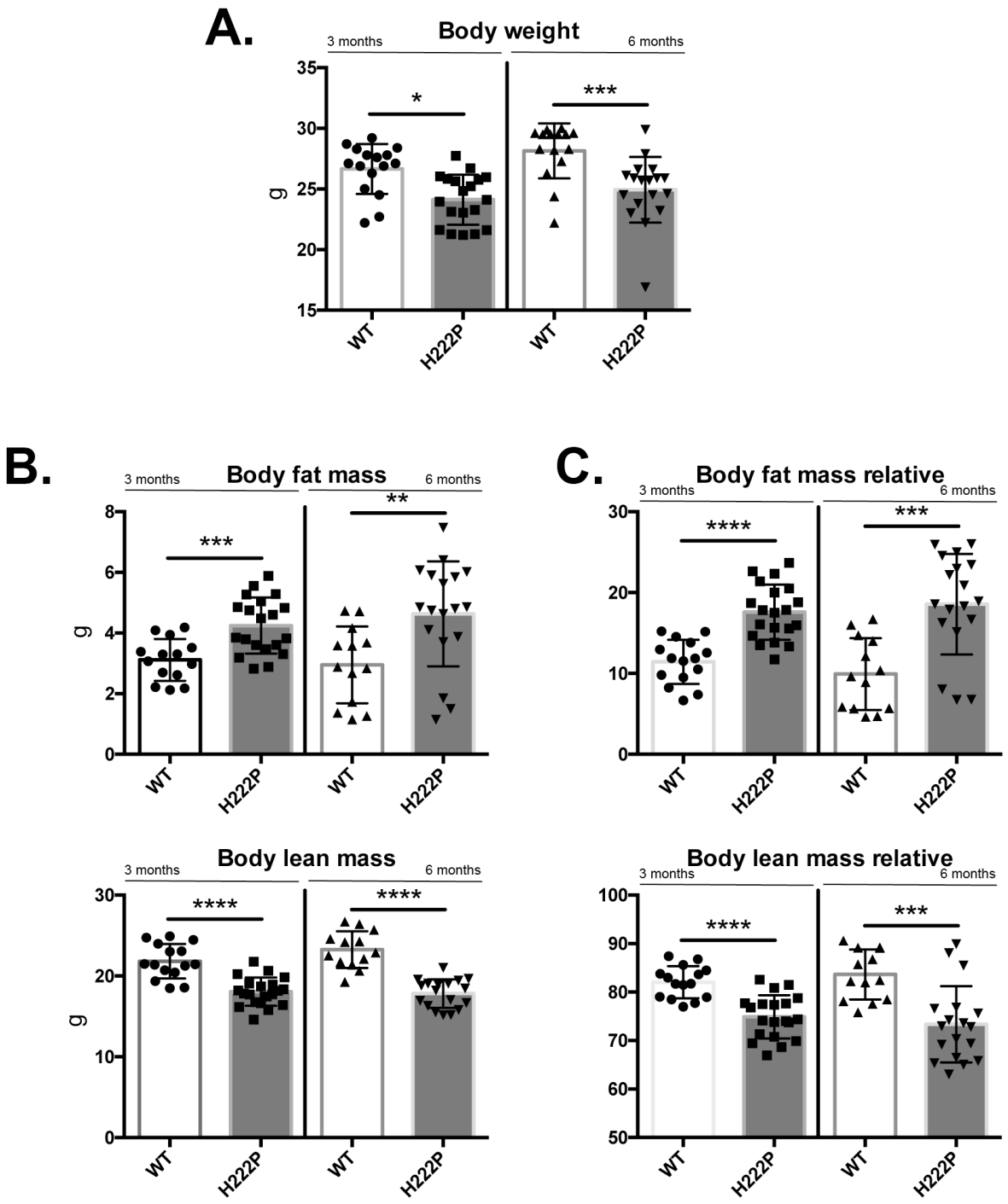

Figure 2. Alteration of body composition in *Lmna*$^{H222P/H222P}$ mice

(A) Graphs showing mean body weight (BW, g) in 3-month-old and 6-month-old male *Lmna*$^{H222P/H222P}$ (H222P) (n=16 at 3 months of age and n=20 at 6 months of age) and wild type (WT) mice. Values for each individual mouse as well SEMs of means (bars) are shown. $^{*}P<0.05$, $^{***}P<0.0005$. **(B)** Graphs showing mean body fat mass (g) and body fat mass relative to BW in 3-month-old and 6-month-old male *Lmna*$^{H222P/H222P}$ (H222P) (n=16 at 3 months of age and n=20 at 6 months of age) and wild type (WT) mice.

Values for each individual mouse as well SEMs of means (bars) are shown. $^{**}P<0.005$, $^{***}P<0.0005$, $^{****}P<0.00005$. **(C)** Graphs showing mean body fat mass (g) and body fat mass relative to BW in 3-month-old and 6-month-old male *Lmna*$^{H222P/H222P}$ (H222P) (n=16 at 3 months of age and n=20 at 6 months of age) and wild type (WT) mice. Values for each individual mouse as well SEMs of means (bars) are shown. $^{***}P<0.0005$, $^{****}P<0.00005$.

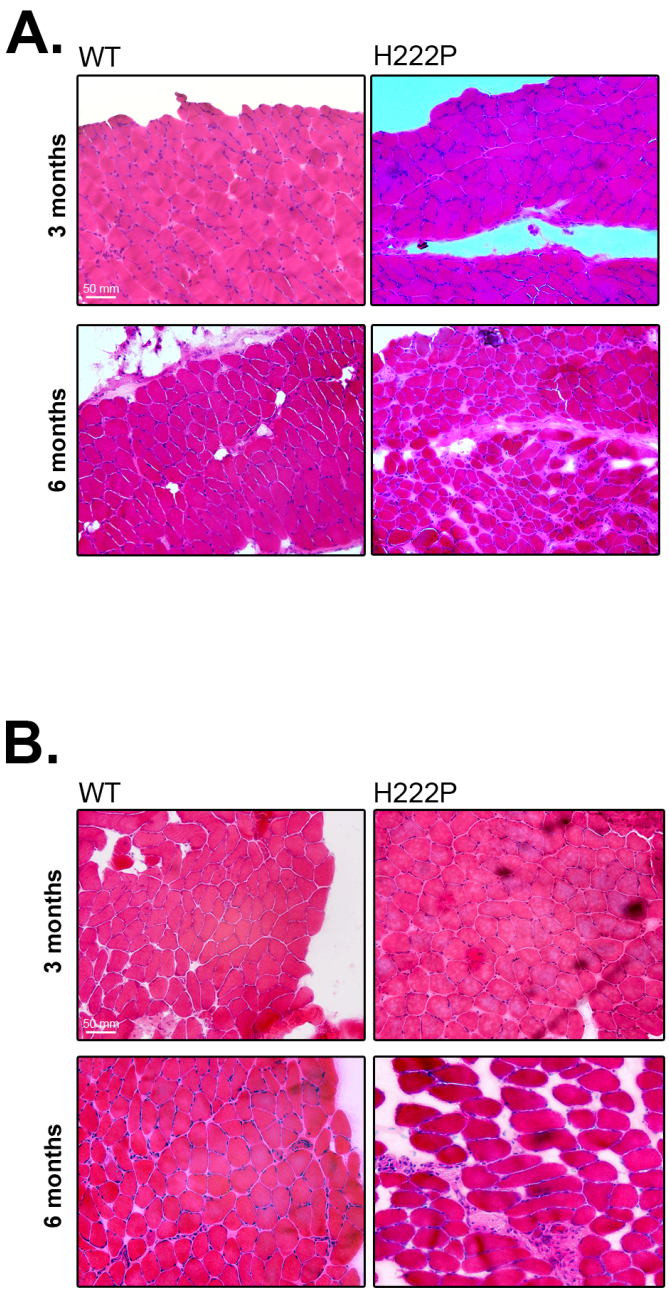

Figure 3. Dystrophic skeletal muscles in *Lmna*$^{H222P/H222P}$ mice
Hematoxylin-Eosin staining of cross sections of diaphragm **(A)** and soleus **(B)** from 3 and 6-month-old male *Lmna*$^{H222P/H222P}$ (H222P) and wild type (WT) mice.

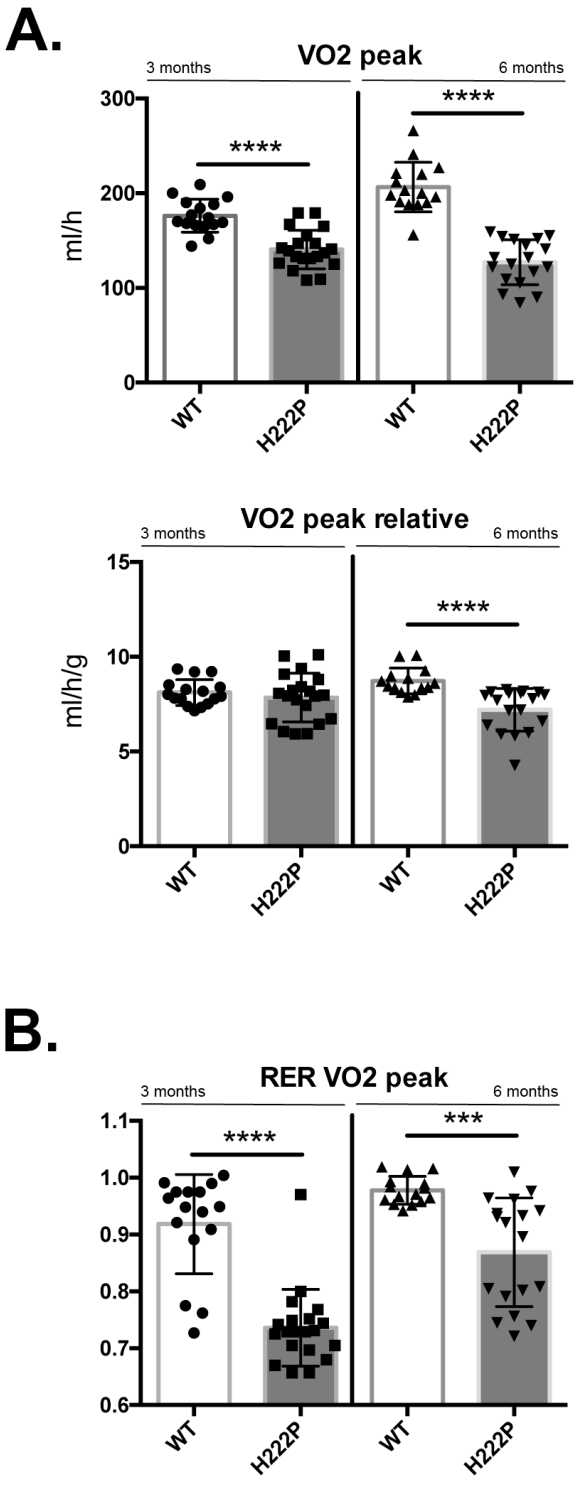

Figure 4. Alteration of maximal performance in *Lmna*$^{H222P/H222P}$ mice

(A) Graphs showing oxygen consumption (VO_2) peak (ml/h) and VO_2 relative to lean mass (ml/h/g) in 3-month-old and 6-month-old male *Lmna*$^{H222P/H222P}$ (H222P) (n=16 at 3 months of age and n=20 at 6 months of age) and wild type (WT) mice. Values for each individual mouse as well as means (histograms) and SEMs of means (bars) are shown. $^{****}P<0.00005$. **(B)** Graphs showing respiratory exchange ratio (RER) at VO_2 peak in 3-month-old and 6-month-old male *Lmna*$^{H222P/H222P}$ (H222P) (n=16 at 3 months of age and

n=20 at 6 months of age) and wild type (WT) mice. Values for each individual mouse as well as means (histograms) and SEMs of means (bars) are shown. $^{***}P<0.0005$, $^{****}P<0.00005$.

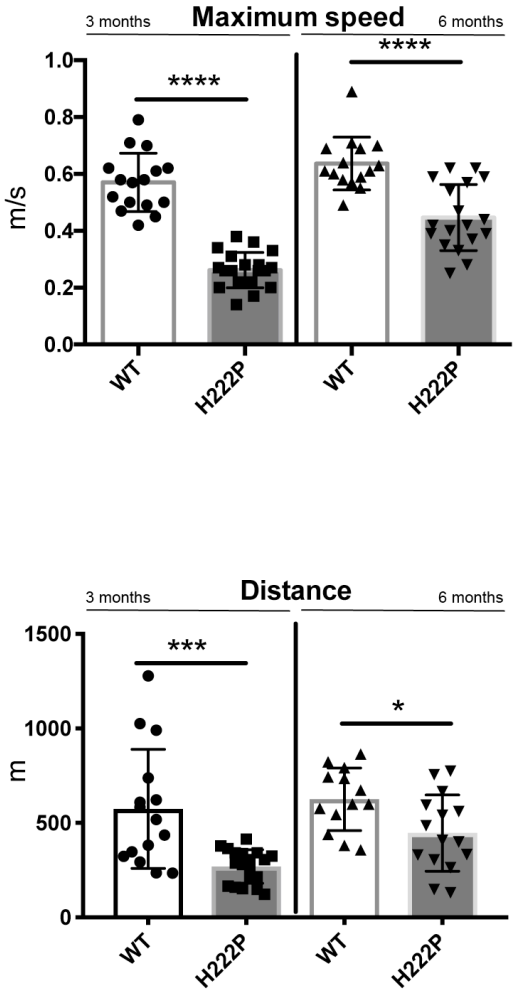

Figure 5. Alteration of physical performance in *Lmna*$^{H222P/H222P}$ mice

Graphs showing mean maximal speed (m/s) and distance (m) in 3-month-old and 6-month-old male *Lmna*$^{H222P/H222P}$ (H222P) (n=16 at 3 months of age and n=20 at 6 months of age) and wild type (WT) mice. Values for each individual mouse as well SEMs of means (bars) are shown. $^{*}P<0.05$, $^{***}P<0.0005$, $^{****}P<0.00005$.

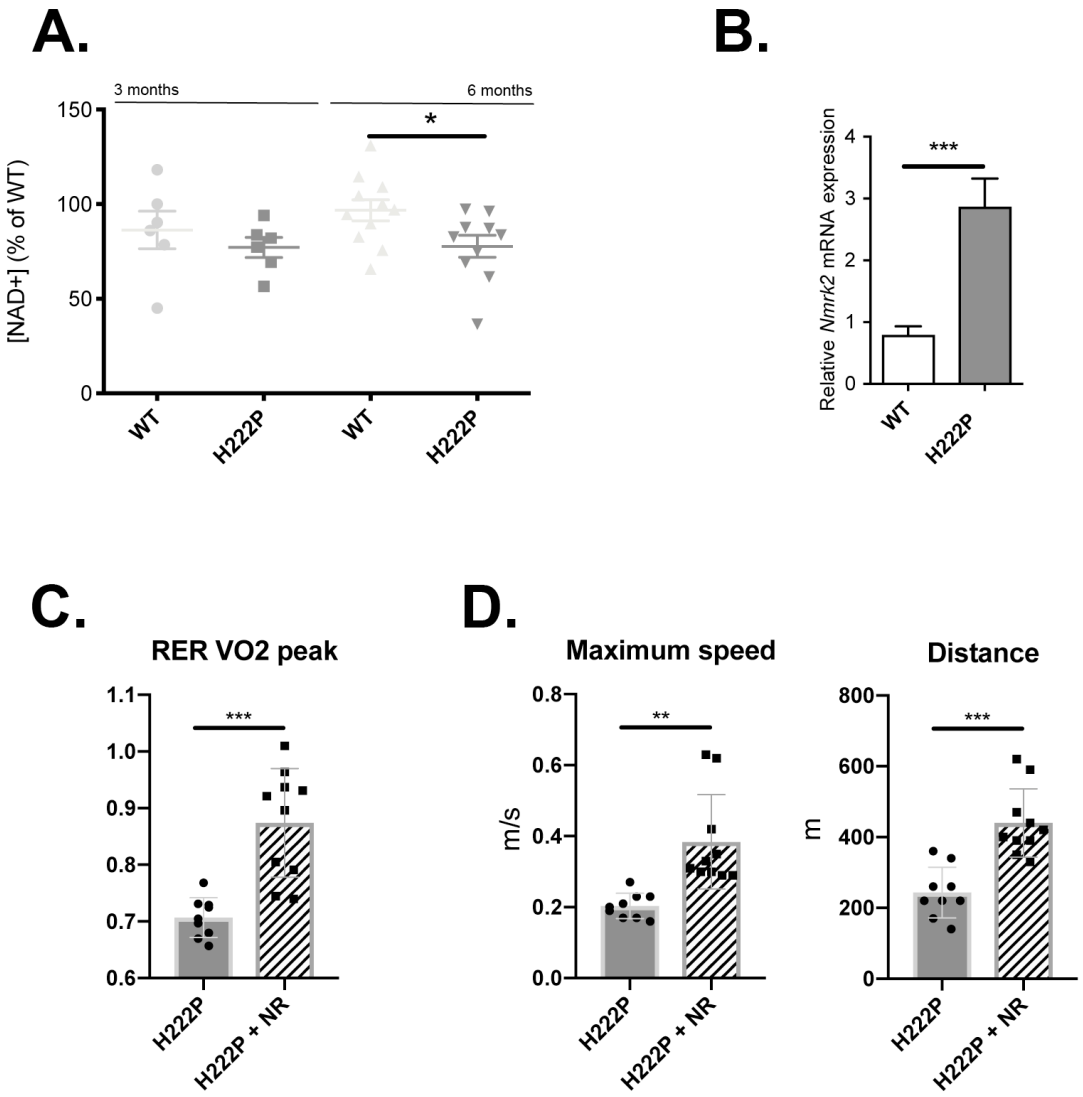

Figure 6. Nicotinamide riboside supplementation leads to improvement of performance in *Lmna*$^{H222P/H222P}$ mice

(A) Quantification of NAD^+ content in soleus from wild type (WT) (n = 6) and *Lmna*$^{H222P/H222P}$ (n=6) mice at 3 and 6 months of age. **P*<0.05. **(B)** Expression of *Nmrk2* mRNA obtained by qPCR from wild type (WT) (n=5) and *Lmna*$^{H222P/H222P}$ (n=5) mice at 6 months of age. ****P*-value < 0.0005. **(C)** Graphs showing respiratory exchange ratio (RER) at VO_2 peak in 6-month-old male chow diet-fed (n=9) or NR-fed *Lmna*$^{H222P/H222P}$ (H222P) (n=10). Values for each individual mouse as well as means (histograms) and SEMs of means (bars) are shown. ***P*<0.005, ****P*<0.0005. **(D)** Graphs showing

mean maximal speed (m/s) and distance (m) in 6-month-old male chow diet-fed (n=9) or NR-fed *Lmna*$^{H222P/H222P}$ (H222P) (n=10). Values for each individual mouse as well SEMs of means (bars) are shown. $^{***}P<0.0005$, $^{****}P<0.00005$.